An Expansion Method for Boundary Layers on Thin Airfoils[1])

By Bernard Grossman[2]) and Stanley G. Rubin, Polytechnic Institute of Brooklyn, Farmingdale, New York, USA

1. Introduction

The laminar incompressible flow over a thin airfoil represents a fundamental problem of fluid mechanics. The inviscid incompressible flow over two-dimensional bodies whose presence only slightly disturbs an initial uniform flow has been studied extensively. Modern analyses such as those by Lighthill [1], Jones and Cohen [2] and Van Dyke [3] present systematic and orderly treatments of this problem.

The associated viscous flow problem has been considered by a variety of methods. These techniques consist of 'similar' solutions, series expansion methods and approximate methods based on integral forms of the equations. Thorough discussion of these techniques can be found in Schlichting [4] and Rosenhead [5].

The objective of the present study is the development of a systematic method for examining the boundary-layer flow over thin symmetric bodies, whose inviscid flow field is specified with the use of small disturbance theory; i.e., a perturbation method for the treatment of rather general flows having small streamwise pressure gradients.

The inviscid flow field is determined as a perturbation of the undisturbed stream and represented by a series of terms in increasing powers of ε, a small thickness parameter. The boundary-layer solution is then formulated as a series expansion in ε and matched, term by term, to the inviscid flow. The boundary-layer solution for any order in ε is found by a quasi-similarity approximation based on the exact functional form of the inviscid flow at the outer edge of the boundary layer. In order that quasi-similarity methods apply, only specific forms of the outer flow may be considered and these will be discussed in detail in Section 2. On the other hand, more general flows can be considered using expansion methods for which the rate of convergence is quite rapid. In Section 3 the effects of higher-order terms (in ε) on the boundary-layer solution are considered. In this connection, the effects of bluntness must be examined.

Perturbation methods, of the type considered here, have previously been used by Mager [6] and Wood [7][3]) to examine the effects of small deviations from uniformity

[1]) This research was supported by the Air Force Office of Scientific Research under Contract No. AF 49(638)-1623, Project No. 9781-01, and under Grant No. AFOSR 70-1843.

[2]) Currently at Grumman Aerospace Corporation, Bethpage, New York. Part of this work is based on a dissertation submitted to the Polytechnic Institute of Brooklyn in partial fulfillment of the requirements for the degree of Doctor of Philosophy (Astronautics).

[3]) The authors would like to thank the reviewer who made them aware of these related investigations.

in the free stream. They both were concerned with small three-dimensional cross-flows and only considered the first-order term in the perturbation expansion. Wood also discussed the first-order solution for two-dimensional thin airfoils using power series expansions to describe a general body shape. He examined the region near a blunt leading edge and noted the relation to the flow over a parabola, which has been discussed more recently by Van Dyke [3]. The present paper explores the matching of the leading-edge solution, which to first-order for a blunt body is approximated by the flow over a parabola, and the thin-airfoil expansion downstream. An example of a body with a sharp leading edge is also discussed in Section 3.

The accuracy of the techniques to be developed in this paper will be illustrated by considering several examples and comparing with other known solutions. It will be shown that good results are obtainable with one or at most two terms in the expansion. The use of this technique for three-dimensional flows, where other two-dimensional methods cannot be applied easily, prompted the considerations presented herein. One such application is discussed in Ref. [8].

2. Inviscid Flow and First-Order Boundary Layer

The inviscid, incompressible flow over a symmetric thin airfoil is considered first. The basic approach to this problem is well documented and may be found in several references, notably Van Dyke [3].

The shape of the airfoil as given in Figure 1 is represented by

$$y_b = y_b(x) = \varepsilon F(x) , \text{ for } 0 \leqslant x \leqslant 1 , \tag{2.1}$$

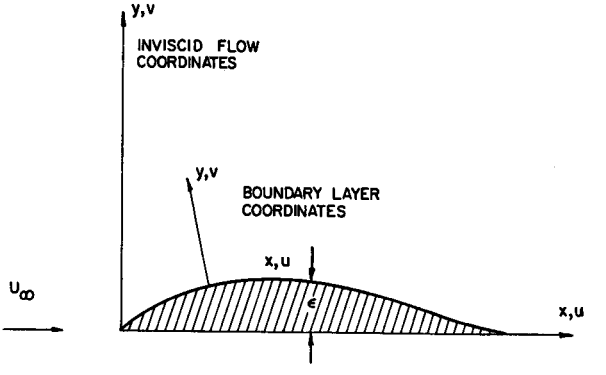

Figure 1
Two-dimensional flow coordinate systems.

where the thickness parameter $\varepsilon \ll 1$, and all lengths have been non-dimensionalized with respect to the chord length c of the airfoil. In terms of a non-dimensional potential function defined by $q = U_\infty \nabla\varphi$ we obtain, as the governing equation for the inviscid flow.

$$\nabla^2\varphi = 0 . \tag{2.2a}$$

From the tangency condition at the body,

$$\frac{\partial\varphi}{\partial n} = 0 \text{ on } y_b = \varepsilon F(x) , \; 0 \leqslant x \leqslant 1 , \tag{2.2b}$$

with symmetry across $y = 0$, for all other values of x; n is the direction of the outward normal to the body. The conditions of uniform flow at infinity is prescribed by

$$\nabla\varphi \to \hat{i}_x, \text{ as } (x^2 + y^2)^{1/2} \to \infty , \tag{2.2c}$$

where $\hat{i}_x$ is a unit vector in the stream direction.

The velocity potential is now assumed to possess an asymptotic expansion in powers of ε of the form

$$\varphi(x, y; \varepsilon) = \sum_{i=0}^{\infty} \varphi_i(x, y)\, \varepsilon^i .$$

The potential problem (2.2a, b, c) may be solved using the well-known techniques of inviscid, thin-airfoil theory. A detailed description of some of these methods are found in Ref. [3].

The velocity along the body surface is designated as $U_e = U_e(x, y_b(x))$, and represents the outer limit for the boundary-layer analysis. It is seen that [3]

$$U_e = 1 + \varepsilon\, \varphi_{1x}(x, 0) + \varepsilon^2 [\varphi_{2x}(x, 0) + F(x)\, F''(x) + 1/2\, F'^2(x)] + O(\varepsilon^3) . \tag{2.3}$$

As a result of the small disturbance solution of the outer flow, $\varphi_1(x, 0)$ is prescribed. The external velocity (2.3), for a large variety of airfoil configurations, will be of the form

$$U_e = 1 + \varepsilon [B_0 \log x + B_1(x \log x) + C_0 + C_1 x + C_2 x^2 + \ldots + C_n x^n] + 0(\varepsilon^2) , \tag{2.4}$$

where B_0, B_1 and C_n are known constants and the coordinate x is now measured along the body surface[4]).

At this point, we are considering only those potential flows having velocity distributions shown in (2.4). In the subsequent discussion, modifications to include terms of the type $\log(1 - x)$ will be discussed. In the following section concerned with second-order theory, the effects of leading-edge bluntness leads to the inclusion of x^{-1} terms in (2.4).

It should be noted that the somewhat artificial external flow $U_e = 1 - \varepsilon\, x$, although not generated by any simple airfoil shape, is a special case of (2.4). For this particular surface speed the present perturbation technique reduces to the well-known Howarth expansion (see Rosenhead [5]).

Introducing the two-dimensional stream function in non-dimensional form

$$\frac{u}{U_\infty} = \psi_Y \text{ and } \frac{v}{U_\infty} = -\psi_x \tag{2.5}$$

into the governing Navier-Stokes equations (e.g., see Rosenhead [5]), and appropriately developing Prandtl's boundary-layer equations (Van Dyke [3]), we obtain the

[4]) Equation (2.4) is unchanged to $O(\varepsilon^2)$ when the cartesian coordinate x is replaced by the body surface coordinate x. Since only terms up to $O(\varepsilon^2)$ are discussed herein, no distinction between the two will be considered.

following boundary-layer problem:

$$\psi_{YYY} + \psi_x \psi_{YY} - \psi_Y \psi_{xY} = - U_e U_e'(x) , \tag{2.6}$$

with the surface conditions

$$\psi(x, 0) = \psi_Y(x, 0) = 0 ,$$

and the outer matching conditions

$$\psi_Y(x, Y) \to U_e(x) \text{ as } Y \to \infty .$$

Here Y is the stretched coordinate normal to the body such that $Y = y\sqrt{Re}$ and the free-stream Reynolds number is defined as $Re = \varrho_\infty U_\infty c/\mu_\infty$.

An asymptotic expansion of ψ is assumed of the form

$$\psi(x, Y; \varepsilon) = \psi^0(x, Y; \log\varepsilon) + \varepsilon \psi^1(x, Y; \log\varepsilon) + O(\varepsilon^2) , \tag{2.7}$$

where $\psi^i(x, Y; \log\varepsilon) = \sum_{n=0}^{k} \psi_{i\,n}(x, Y) (\log\varepsilon)^n$ and $\psi_{i\,0}(x, Y)$ is designated as $\psi_i(x, Y) \equiv \psi_i$.

This allows for the possible inclusion of logarithmic terms in the expansion. Such terms may result from leading-edge effects, the appearance of eigenfunctions in the perturbation scheme or a combination thereof. Substituting this expansion into (2.6) and retaining terms of 0(1) we find that the solution is the well-known Blasius function (cf. Rosenhead [5]), where

$$\psi_0 = \sqrt{2x}\, f(\eta); \quad \eta = \frac{Y}{\sqrt{2x}} ; \tag{2.8}$$

and

$$f'''(\eta) + f(\eta) f''(\eta) = 0 , \tag{2.9}$$

with

$$f(0) = f'(0) = 0 \qquad f'(\infty) = 1 .$$

The Blasius solution may be found tabulated on page 223 of Ref. [5].

The governing equations to first order in ε are obtained in a similar manner. Defining a (ξ, η) coordinate system, where $\xi = x$, $\eta = Y/\sqrt{2x}$ and ψ_0 is given by (2.8), the first-order equations become

$$\psi_{1\,\eta\eta\eta} + f(\eta) \psi_{1\,\eta\eta} + f'(\eta) \psi_{1\,\eta} + 2\xi [f''(\eta) \psi_{1\,\xi} - f'(\eta) \psi_{1\,\eta\xi}] =$$
$$- [B_0/\xi + B_1 \log\xi + (B_1 + C_1) + 2 C_2 \xi + \cdots + n C_n \xi^{n-1}] 2\xi \sqrt{2\xi} , \tag{2.10}$$

with

$$\psi_1(\xi, 0) = \psi_{1\,\eta}(\xi, 0) = 0 ,$$

and

$$\lim_{\eta\to\infty} \psi_{1\,\eta}(\xi, \eta) = B_0 \log\xi + B_1 \xi \log\xi + C_0 + C_1 \xi + C_2 \xi^2 + \cdots + C_n \xi^n . \tag{2.11}$$

By analogy with the methods used in obtaining 'similar' boundary-layer solutions and utilizing the linearity of (2.10), we choose ψ_1 to be of the following quasi-similar form:

$$\psi_1(\xi, \eta) = \sqrt{2\,\xi}\,[B_0 \log\xi\, M_0(\eta) + B_1\,\xi \log\xi\, M_1(\eta) + C_0\, N_0(\eta) + C_1\,\xi\, N_1(\eta) + C_2\,\xi^2\, N_2(\eta) + \cdots + C_n\,\xi^n\, N_n(\eta)]\,, \tag{2.12a}$$

where

$$M_0(0) = M_1(0) = N_n(0) = M_0'(0) = M_1'(0) = N_n'(0) = 0\,, \tag{2.12b}$$

and

$$\lim_{\eta\to\infty} M_0'(\eta) = M_1'(\eta) = N_n'(\eta) = 1\,.$$

Substituting (2.12a) into (2.10) and noting that ξ and η are independent, we obtain the following ordinary differential equations:

$$M_0''' + f\,M_0'' + f''\,M_0 = 0\,, \tag{2.13a}$$

$$M_1''' + f\,M_1'' - 2\,f'\,M_1' + 3\,f''\,M_1 = -2\,, \tag{2.13b}$$

$$N_0''' + f\,N_0'' + f''\,N_0 = \frac{-2\,B_0}{C_0}\,(1 + f''\,M_0 - f'\,M_0')\,, \tag{2.13c}$$

$$N_1''' + f\,N_1'' - 2\,f'\,N_1' + 3\,f''\,N_1 = -2 - \frac{2\,B_1}{C_1}\,(1 + f''\,M_1 - f'\,M_1')\,, \tag{2.13d}$$

and for $n \geqslant 2$

$$N_n''' + f\,N_n'' - 2\,f'\,N_n' - 2\,n\,f'\,N_n' + (1 + 2\,n)\,f''\,N_n = -2\,n\,. \tag{2.13e}$$

The solution of these equations, subject to the boundary conditions (2.12b), represent the first-order (ε) boundary-layer effect. In addition to the solution depicted in (2.12a), equation (2.10) has a countable set of eigensolutions (cf. Stewartson [9], Libby and Fox [10]) that should be added to (2.12a). However, these solutions are singular as $\xi \to 0$ and by matching with a local solution at the leading edge it will be shown in Section 3 that the eigensolution of $0(\xi^{-n})$ first enters into the expansion (2.7) when terms of $0(\varepsilon^{2n})$ are considered. Since the lowest value of n is unity [9, 10], we would expect contribution in the ε^2 term.

It is of interest to note that only equations (2.13c) and (2.13d) depend on the coefficient B_0, B_1, C_0 and C_1. Hence, the other equations may be solved in general. Typical solutions are given in Table A-1. In addition, it can be seen that the solution to equation (2.13a) is

$$M_0 = 1/2\,[f(\eta) + \eta\,f'(\eta)]\,. \tag{2.14}$$

For future reference the non-dimensional shear stress at the wall, $\eta = 0$ is prescribed

in general by

$$\left.\begin{aligned}\frac{C_f}{2}\sqrt{R_{e_\infty}} = \psi_{YY}(x,0) = \psi_{0YY}(x,0) + \varepsilon\,\psi_{1YY}(x,0) = \frac{1}{\sqrt{2x}}\,f''(0) \\ + \frac{\varepsilon}{\sqrt{2x}}\,[B_0 \log x\, M_0''(0) + B_1\, x \log x\, M_1''(0) + C_0\, N_0''(0) \\ + C_1\, x\, N_1''(0) + \ldots + C_n\, x^n\, N_n''(0)]\,.\end{aligned}\right\} \tag{2.15}$$

Specific applications of this first-order viscous small-disturbance theory now are considered. The method is first applied to a thin Joukowski airfoil which is illustrative of the class of problems whose velocity at the outer edge of the boundary layer is of the form given by (2.4). A second application is that of a slender parabolic-arc airfoil where an additional coordinate expansion is necessary in order that the methods described herein are directly applicable.

Joukowski Airfoil

We consider a thin symmetrical Joukowski airfoil whose shape to first order is given by

$$y = 2\,\varepsilon\,(1-x)\sqrt{x\,(1-x)} \tag{2.16}$$

where here ε is 0.769 times the maximum thickness ratio. With (2.16), and from (2.3), and Van Dyke [3], the velocity external to the boundary layer becomes

$$U_e = 1 + \varepsilon\,(3 - 4\,x)\,. \tag{2.17}$$

In accordance with (2.4), the constants are prescribed as follows:

$$B_0 = B_1 = 0;\ C_0 = 3;\ C_1 = -4;\ C_i = 0,\ i \geqslant 2\,.$$

From (2.12a), the boundary-layer solution becomes

$$\psi_Y = f'(\eta) + \varepsilon\,[3\,N_0'(\eta) - 4\,x\,N_1'(\eta)]\,, \tag{2.18}$$

where $N_0 = M_0$ and $N_1 = M_1$, as defined by (2.12a), (2.13b) and (2.14). (See Ref. [13] for details.)

The shear stress along the body from (2.15) is

$$\frac{C_f}{2}\sqrt{R_{e_\infty}} = \frac{1}{\sqrt{2x}}\,\{f''(0) + \varepsilon\,[3\,M_0''(0) - 4\,x\,M_1''(0)]\}\,, \tag{2.19}$$

where $f''(0) = 0.4696$, $M_0'' = 0.7044$, $M_1''(0) = 2.890$. The velocity profiles and the shear stress distribution are plotted for various values of x and ε in Figures 2, 3 and 4.

Figure 2 depicting the velocity profiles shows that the deviations from the flat plate profile increase moderately as the body thickness (ε) increases, while Figures 3 and 4 depict the decrease in $u_\eta(x, 0)$ for increasing values of x. The figures also indicate that separation occurs on the airfoil. The location of the separation point is seen to propagate upstream with increasing values of ε, as would be expected.

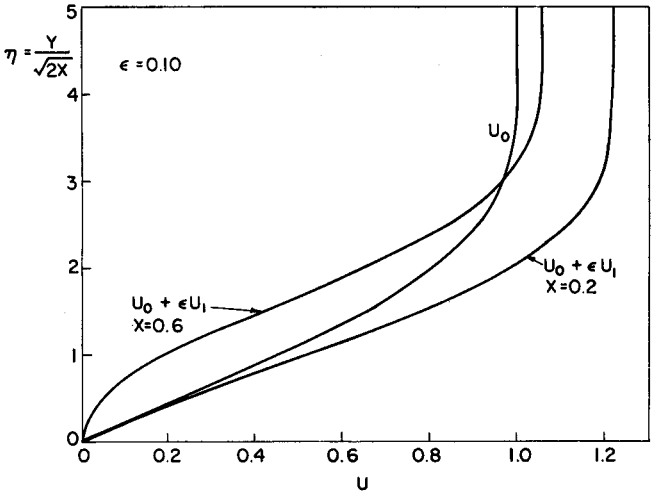

Figure 2
Velocity profile, Joukowski airfoil.

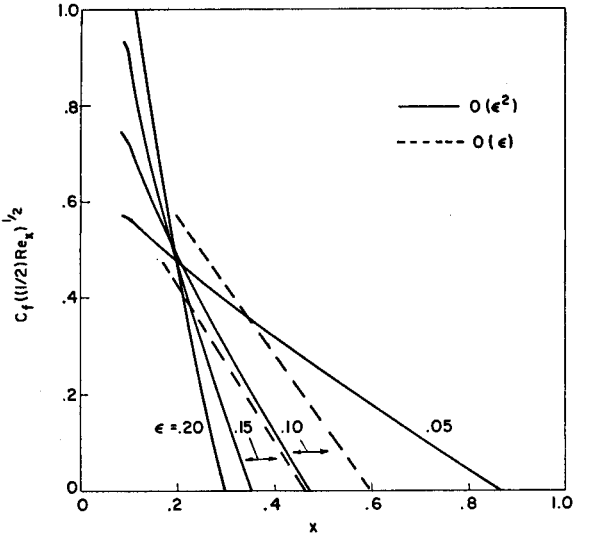

Figure 3
Non-dimensional skin friction vs. x, Joukowski airfoil.

It is important to note that the potential flow analysis discussed herein is obtained for a non-separated flow and therefore, any solutions presented should not be valid after separation has occurred. Furthermore, the nature of the flow in the vicinity of the separation point is improperly described by the present perturbation scheme. However, there is experimental evidence showing that for the slender airfoils considered here, the flow solutions derived should be reasonably good upstream of the separation point and may be useful in approximating the position of the separation point. These facts are again discussed in Section 3 in connection with higher-order solutions of the Joukowski airfoil.

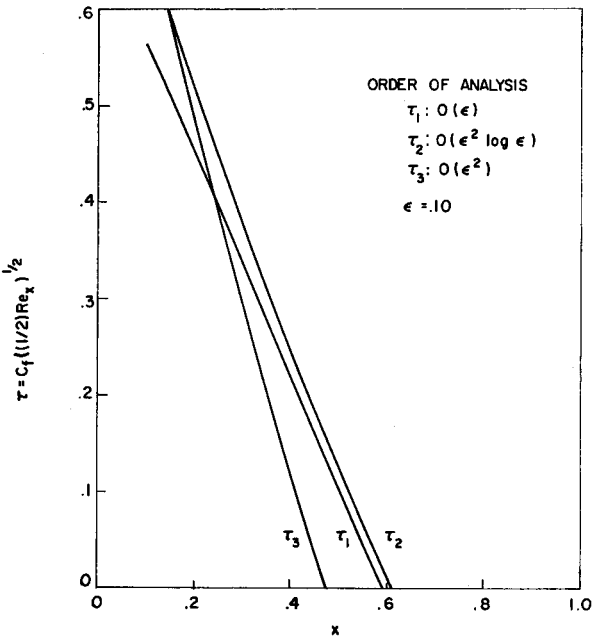

Figure 4
Non-dimensional skin friction vs. x, Joukowski airfoil.

Parabolic-Arc Airfoil

As a second example, consider a symmetric airfoil formed by the intersection of two parabolic arcs such that

$$y = 4\,\varepsilon\,(x - x^2)\,.$$

For this case, the inviscid potential flow solution is

$$U_e = 1 + \frac{4\,\varepsilon}{\pi}\,[2 - (1 - 2\,x)\log(1 - x) + (1 - 2\,x)\log x]\,. \tag{2.20}$$

We find that typical of small-disturbance solutions a singularity appears at the leading edge $x = 0$.

To obtain U_e in the form given by (2.4) so that 'quasi-similarity' solutions are possible, it is necessary to expand the $\log(1 - x)$ term in (2.20) for small values of x such that

$$\log(1 - x) = -\,x - \frac{x^2}{2} - \frac{x^3}{3} - \cdots \frac{-\,x^n}{n} \cdots\,. \tag{2.21}$$

Substituting (2.21) into (2.20) we find that

$$U_e = 1 + \frac{4\,\varepsilon}{\pi}\left[\log x - 2\,x\log x + 2 + x - \frac{3\,x^2}{2} - \frac{2\,x^3}{3} - \cdots\right]. \tag{2.22}$$

Therefore, in accordance with equation (2.4), $B_0 = 4/\pi$, $B_1 = -8/\pi$, $C_0 = 8/\pi$, $C_1 = 4/\pi$ and $C_n = [-4\,(n + 1)]/[\pi\,n\,(n - 1)]$ for $n \geqslant 2$. Using the techniques developed

in this section, the velocity profile in the boundary layer is

$$u = \psi_Y = \sqrt{2x}\left\{ f'(\eta) + \frac{4\varepsilon}{\pi}\left[M_0'(\eta)\log x - 2M_1'(\eta)\, x \log x \right.\right.$$
$$\left.\left. + 2\bar{N}_0'(\eta) + \bar{N}_1'(\eta)\, x - \sum_{n=2}^{\infty} \frac{(n+1)}{n(n-1)} x^n N_n'(\eta)\right]\right\} . \qquad (2.23)$$

The only ordinary differential equations not previously discussed are

$$\bar{N}_0''' + f\bar{N}_0'' + f''\bar{N}_0 = -(1 + f''M_0 - f'M_0'),$$
$$\bar{N}_0(0) = \bar{N}_0(0) = 0, \quad \bar{N}_0'(\infty) = 1, \qquad (2.24a)$$

$$\bar{N}_1''' + f\bar{N}_1'' - 2f'\bar{N}_1' + 3f''\bar{N}_1 = -2 + 4(1 + f''M_1 - f'M_1'),$$
$$\bar{N}_1(0) = \bar{N}_1(0) = 0, \quad \bar{N}_1'(\infty) = 1. \qquad (2.24b)$$

Numerical solutions for these equations are presented in Table A-1. We recall that $\bar{N}_0$ and $\bar{N}_1$ depend explicitly on the form of the external flow. The $N_n(\eta)$ $(n > 1)$ are universal functions and can be tabulated; series expansions of the type (2.23) can then be evaluated to any reasonable degree of accuracy.

The solution of (2.23) is evaluated by including a finite number of terms in the coordinate expansion for $\log(1 - x)$ and is truncated after the x^4 term. To this approximation U_e should be accurate to within 5% of its value as given by (2.20), for $0.1 \leqslant x \leqslant 0.85$, $0 \leqslant \varepsilon \leqslant 0.4$. The solution is not valid at the leading edge where it is singular. Velocity profiles at various streamwise locations, and for selected values of ε are shown in Figure 5. From the curve depicting the skin friction (Fig. 6), it can be seen that the separation point is within the range of x for which the solution should

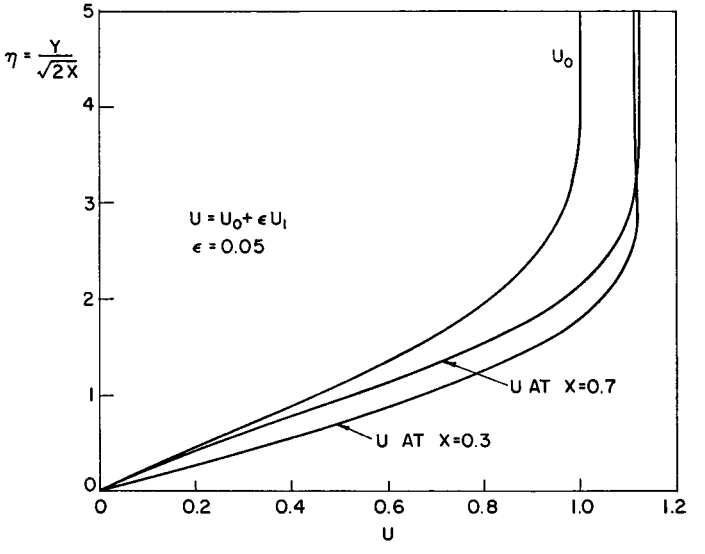

Figure 5
Velocity profile, parabolic arc.

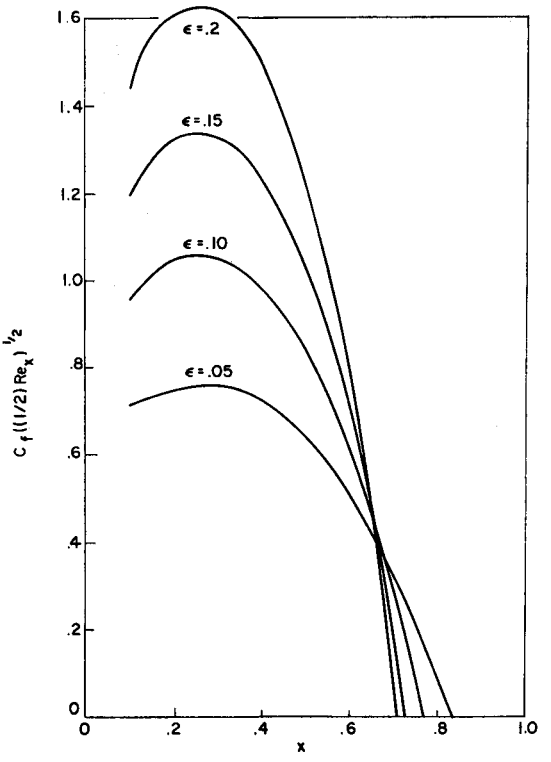

Figure 6
Skin friction vs. x, parabolic arc.

be acceptable and that over a range of values of thickness parameter of 0.05 to 0.20 the laminar separation point only varies from 0.83 to 0.71.

3. Second-Order Theory and Eigensolutions

From the previous analysis it is seen that the potential flow over a thin Joukowski airfoil is singular at the leading edge. This condition is typical for blunt-nosed airfoils, and the correction to the potential flow is discussed by Van Dyke [11]. Although the leading-edge potential flow does not directly affect the analysis for the flow downstream of $x > 0(\varepsilon^2)$, in that small-disturbance theory is valid on this range, it is found that an eigensolution in the downstream boundary-layer solution leads to an arbitrary constant which must be determined by matching with the leading-edge boundary layer. It will be shown that the effect of a blunt leading edge on the boundary layer will not appear until order $\varepsilon^2 \log \varepsilon$ so that the first-order (ε) boundary layer developed in the previous section remains unchanged.

Any singularities occurring at the leading edge of a sharp-nosed airfoil are so weak as to have a negligible effect on the flow downstream of $x > 0(e^{-1/\varepsilon})$ (see Van Dyke [3, 11]).

The procedure for determining the effect of leading-edge bluntness on the potential flow field for a Joukowski airfoil has been considered by Van Dyke [3] by examining the flow near the leading edge, where $S = x/2\,\varepsilon^2$ is of 0(1). The boundary-

layer solution near the leading edge has also been treated by Van Dyke [11]. From the asymptotic matching principle the limiting values as $S \to \infty$ must match the boundary-layer solution obtained herein as $x \to 0$.

Consider the stretched coordinates

$$\bar{y} = \frac{y}{2\,\varepsilon^2}\,, \qquad S = \frac{x}{2\,\varepsilon^2}\,. \tag{3.1}$$

In these variables, with the limit $\varepsilon \to 0$, keeping S fixed, the airfoil shape is of the form

$$\bar{y} = \sqrt{2\,S}\,[1 + O(\varepsilon^2)]\,. \tag{3.2}$$

The inviscid solution for this parabolic body gives

$$U_e = \sqrt{2\,S}\,[1 + \varepsilon + O(\varepsilon^2)]\,. \tag{3.3}$$

The leading term in (3.2) corresponds to the flow over an infinite parabola. The boundary layer on this body has been determined by Van Dyke [11] using a Blasius-Howarth series-expansion technique (cf. Rosenhead [5]) near the nose and a supplementary expansion technique valid downstream for large S which he denoted as an 'inverse Blasius series'. In terms of the non-dimensional skin friction coefficient, this solution, valid downstream of the nose of the parabola, i.e., for large S, is:

$$(1/2\,Re_x)^{1/2}\,C_f = 0.469600\left[1 + 0.60115\,\frac{1}{2\,S}\log 2S + \frac{0.89}{S}\right],$$

where $Re_x = U_\infty\,x/\nu_\infty$. The constant 0.89 in the above equation was obtained by Van Dyke [11] by matching to the series solution in the vicinity of the nose of the parabola. Rewriting the above equation in terms of the physical coordinate x, it is found that:

$$(1/2\,Re_x)^{1/2}\,C_f = 0.469600\,[1 - 0.60115\,\frac{2\,\varepsilon^2}{x}\log\varepsilon + \frac{\varepsilon^2}{x}(0.89 + 0.60115\,\log x)]\,. \tag{3.4}$$

This equation represents the leading term of the zero-order asymptotic expansion in ε. The $\varepsilon^2\log\varepsilon$ and ε^2 term appear as a result of the stretching. It can be seen that the higher-order terms cannot generate any additional contributions of the form $\varepsilon^2/x\log\varepsilon$, ε^2/x or $\varepsilon^2/x\log x$. This fact will be utilized in the following analysis.

With consideration of the form of the solution near the nose of the airfoil, the stream function (2.7) is expanded as

$$\psi = \psi_0 + \varepsilon\,\psi_1 + \varepsilon^2\log\varepsilon\,\psi_{21} + \varepsilon^2\,\psi_2 + \ldots\,. \tag{3.5}$$

The inclusion of the $\varepsilon^2\log\varepsilon$ term is necessary in order that (2.15) match with the upstream solution (3.4). This $\varepsilon^2\log\varepsilon$ term ψ_{21} is seen to correspond to the lowest eigensolutions discussed previously and the associated constant must be determined by matching to the solution valid near the nose.

We have previously determined that

$$\psi_0 = \sqrt{2\,x}\,f(\eta); \qquad \psi_1 = \sqrt{2\,x}\,[3\,N_0(\eta) - 4\,x\,N_1(\eta)]\,.$$

Since no terms of order $\varepsilon^2 \log\varepsilon$ appear in the outer flow, after substituting expansion (3.5) into (2.6) and retaining terms to order $\varepsilon^2 \log\varepsilon$, the governing equation for ψ_{21} becomes

$$\psi_{21\,\eta\eta\eta} + f(\eta)\,\psi_{21\,\eta\eta} + f'(\eta)\,\psi_{21\,\eta} + 2\,\xi\,[f''(\eta)\,\psi_{21\,\xi} - f'(\eta)\,\psi_{21\,\xi\eta}] = 0\,, \tag{3.6}$$

with the boundary conditions

$$\psi_{21}(\xi, 0) = \psi_{21\,\eta}(\xi, 0) = 0\,, \quad \psi_{21\,\eta}(\xi, \infty) = 0\,.$$

In accordance with the solution near the nose of the airfoil, it is assumed that

$$\psi_{21} = \frac{\sqrt{2\,\xi}}{\xi}\,K_1(\eta)\,.$$

Substituting into (3.6), the governing equation for K_1 becomes

$$K_1''' + f\,K_1'' + 2\,f'\,K_1 - f''\,K_1 = 0\,, \tag{3.7}$$

with

$$K_1(0) = K_1'(0) = K_1'(\infty) = 0\,.$$

This eigenvalue problem corresponds to the eigenvalue $\lambda = -2$ in the analysis of Libby and Fox [10]. The solution is

$$K_1(\eta) = \alpha_1\,[\eta\,f'(\eta) - f(\eta)] \tag{3.8}$$

where α_1 is a constant whose numerical value will be found by matching to the solution near the nose of the airfoil. Since the next eigensolution is of $0(\xi^{-1.87})$ [10] we would not expect any additional eigensolutions to enter into this analysis which includes only terms up to $0(\varepsilon^2)$. The appearance of eigensolutions in higher-order terms will depend upon the specific nature of the leading-edge flow.

Joukowski Airfoil

For the one specific case of the Joukowski airfoil it is found from (2.3) that the velocity at the edge of the boundary layer to order ε^2 is

$$U_e = 1 + \varepsilon\,(3 - 4\,x) + \varepsilon^2\left(-\frac{1}{2\,x} + \frac{9}{2} - 12\,x + 8\,x^2\right). \tag{3.9}$$

Retaining terms of order ε^2 in the expansion (3.5) of the governing boundary-layer equations (2.6) yields

$$\psi_{2\eta\eta\eta} + f\,\psi_{2\eta\eta} + f'\,\psi_{2\eta} + 2\,\xi\,(f''\,\psi_{2\xi} - f'\,\psi_{2\,\eta\,\xi}) = -\sqrt{2\,\xi}\,\{9\,N_0\,N_0'' + 12\,\xi\,(2\,N_0'\,N_1' - 3\,N_1\,N_0'' - N_0\,N_1'' - 4) + 16\,\xi^2\,(3\,N_1\,N_1'' - 2\,N_1'^2 + 4) + \xi^{-1}\}\,. \tag{3.10}$$

Consistent with the solution near the nose of the airfoil and with the form of the outer flow, to order ε^2, the stream function ψ_2 is assumed to be of the following form:

$$\psi_2 = \sqrt{2\,\xi}\left[-\frac{1}{2\,\xi}\,K_2(\eta) + \frac{\log\xi}{\xi}\,K_3(\eta) + \frac{9}{2}\,L_0(\eta) - 12\,\xi\,L_1(\eta) + 8\,\xi^2\,L_2(\eta)\right]. \tag{3.11}$$

Substituting (3.11) into (3.10), we obtain the following system of ordinary differential equations:

$$K_2''' + f K_2'' + 2 f' K_2' - f'' K_2 = 2 (1 + 2 f'' K_3 - 2 f' K_3') , \tag{3.12a}$$
$$K_2(0) = K_2'(0) = 0, \quad K_2'(\infty) = 1,$$

$$K_3''' + f K_3'' + 2 f' K_3' - f'' K_3 = 0 , \tag{3.12b}$$
$$K_3(0) = K_3'(0) = K_3'(\infty) = 0 ,$$

$$L_0''' + f L_0'' + f'' L_0 = -2 N_0 N_0'' , \tag{3.12c}$$
$$L_0(0) = L_0'(0) = 0, \quad L_0'(\infty) = 1 ,$$

$$L_1''' + f L_1'' - 2 f' L_1' + 3 f'' L_1 = 2 N_0' N_1' - 3 N_1 N_0'' - N_0 N_1'' - 4 , \tag{3.12d}$$
$$L_1(0) = L_1'(0) = 0, \quad L_1'(\infty) = 1 ,$$

$$L_2''' + f L_2'' - 4 f' L_2' + 5 f'' L_2 = -2 (3 N_1 N_1'' - 2 N_1'^2 + 4) , \tag{3.12e}$$
$$L_2(0) = L_2'(0) = 0, \quad L_2'(\infty) = 1 .$$

Solutions of (3.12) give $L''(0) = 1.057$, $L_1''(0) = 4.337$ and $L_2''(0) = 1.365$. Equation (3.12b) is the identical eigenvalue problem as that given by (3.7) so that

$$K_3 = \alpha_3 [\eta f'(\eta) - f(\eta)] , \tag{3.13}$$

where α_3 is a constant. The solution to (3.12a) is written as

$$K_2 = \overline{K} + \alpha_2 [\eta f' - f] , \tag{3.13a}$$

where $\overline{K}$ is the solution of

$$\overline{K}''' + f \overline{K}'' + 2 f' \overline{K}' - f'' \overline{K} = 2 (1 - \alpha_3 f f'') ,$$
$$\overline{K}(0) = \overline{K}'(0) = 0, \quad \overline{K}''(0) = 1 . \tag{3.14}$$

The non-dimensional skin friction at the wall becomes

$$\left.\begin{aligned} (1/2\, Re_x)^{1/2} C_f = {} & f''(0) + \varepsilon [3 M_0''(0) - 4 x N_1''(0)] + \varepsilon^2 \log \varepsilon \frac{\alpha_1}{x} f''(0) \\ & + \varepsilon^2 \left[\left(-\frac{1}{2x} \right) (1 + \alpha_2 f''(0)) + \left(\frac{\log x}{x} \right) \alpha_3 f''(0) + \frac{9}{2} L_0''(0) \right. \\ & \left. - 12 x L_1''(0) + 8 x^2 L_2''(0) \right] . \end{aligned}\right\} \tag{3.15}$$

The constants α_1, α_2 and α_3 will now be determined by asymptotically matching (3.15) to (3.4). Equation (3.4) represents the one term inner solution which, after being written in terms of inner variables, expanded for small ε with S fixed and rewritten in terms of outer variables, is matched to equation (3.15). We thereby, obtain

$$\alpha_1 = -1.202 , \quad \alpha_2 = -5.920 , \quad \alpha_3 = 0.601 .$$

Equation (3.14) may be solved numerically.

The skin friction as a function of the streamwise distance x for various values of ε is shown in Figures 3 and 4. Figure 3 illustrates the effect of airfoil thickness on the position of the separation point; as the airfoil thickness increases, the position of the separation point moves upstream. The effects of higher-order terms on the skin friction are shown in Figure 4. From (3.15) we find that no separation occurs on the airfoil surface for thickness ratios less than 6.5% ($\varepsilon = .05$) to $0(\varepsilon)$ and less than 5.5% ($\varepsilon = .043$) to $0(\varepsilon^2)$. This result compares favorably with the experimental observation of Fage, Falkner and Walker (1929) which shows that a 5% Joukowski airfoil in a laminar flow does not separate (see the discussion on page 109 of Ref. [5]). It is seen that the ε^2 term leads to a substantial correction in the total skin friction in the vicinity of the separation point. This is also seen by considering a Joukowski airfoil with $\varepsilon = 0.092$ corresponding to a maximum thickness of approximately 12%, where it is found that the separation point accurate to $0(\varepsilon)$ is located at $(x/c) = 0.62$, whereas the $0(\varepsilon^2)$ correction reduces the value to $(x/c) = 0.49$. By other techniques [12]; namely, a numerical boundary layer solution using the method of Smith and Clutter, the separation point is found to occur at $x = 0.46$. Hence, the skin friction with terms of order ε^2 predicts the position of the laminar separation point to within 6% of that found by more exact techniques.

Slender Wedge

As a second example of the higher-order theory, the boundary layer on a slender semi-infinite wedge is considered. This problem is particularly significant in that a 'similar' solution of the boundary layer is available which will provide additional insight to the accuracy of the methods described in this paper.

The well-known result for the inviscid flow over this body is

$$U_e = U_1 x^{\beta/(2-\beta)} \tag{3.16}$$

where U_1 is a constant and x is measured along the wedge surface; the included half-angle is $\pi\,\beta/2$. Consistent with the analysis presented herein it is assumed that

$$\varepsilon = \pi\,\beta/2 \ll 1\,. \tag{3.17}$$

The velocity external to the boundary layer, after expanding for small values of ε becomes

$$\frac{U_e}{U_1} = 1 + \frac{\varepsilon}{\pi}\log x + \frac{\varepsilon^2}{2\pi^2}(2\log x + \log^2 x) + \ldots\,. \tag{3.18}$$

It is important to note that the general thin-airfoil techniques presented in the beginning of this paper can be used to find the inviscid flow solution for a thin finite wedge. Since the solution (3.16) relates to an infinite wedge, some limiting process must be considered. This discrepancy is resolved by considering a finite wedge of length a, where a is very large, and also restricting x to be much less than a. From Van Dyke [3]

$$\varphi_{1x} = \frac{1}{2\pi}\int_0^a \frac{-2\,(x'-x)\,dx'}{(x'-x)^2 + y^2} = \frac{1}{2\pi}\log\frac{x^2+y^2}{(a-x)^2+y^2}\,. \tag{3.19}$$

Substituting (3.19) into (2.3) and assuming $a \gg (x^2 + y^2)^{1/2}$, then

$$U_e \sim 1 - \frac{\varepsilon}{\pi} \log a + \frac{\varepsilon}{\pi} \log x + \dots$$

Now defining $U_1 = 1 - \varepsilon/\pi \log a$, we have

$$U_e \sim U_1 [1 + \frac{\varepsilon}{\pi} \log x + O(\varepsilon^2)] ,$$

which is the leading term of the expansion for small β of the local solution for an infinite wedge (3.16). U_1 may now be eliminated from the above equation by non-dimensionalizing all velocities with respect to $U_1\, U_\infty$.

This technique is somewhat analogous to that used by Van Dyke [3] in matching the solution near the nose of a sharp airfoil to the local solution for an infinite wedge. However, we are not considering the local solution at this point.

The boundary-layer solution may now be found as outlined previously. The first-order boundary layer leads to

$$\psi_1 = \sqrt{2\,x} \left[\frac{1}{\pi} \log x \; M_0(\eta) + \frac{1}{\pi} \tilde{N}_0(\eta) \right] , \tag{3.20}$$

where M_0 is governed by (2.20a) and is given as

$$M_0 = 1/2 \, [f(\eta) + \eta \, f'(\eta)]; \tag{3.21}$$

$\tilde{N}_0$ is determined by

$$\tilde{N}_0''' + f \tilde{N}_0'' + f'' \tilde{N}_0 = -2 \, [1 - f'^2 + 1/2 \, f f''] , \tag{3.22}$$

with

$$\tilde{N}_0(0) = \tilde{N}_0'(0) = \tilde{N}_0'(\infty) = 0 .$$

The next term of the expansion of ψ is of the order ε^2. Consistent with (3.18), it is assumed to be of the form:

$$\psi_2 = \sqrt{2\,x} \left[\frac{1}{\pi^2} \tilde{L}_0(\eta) + \frac{1}{\pi^2} \tilde{K}_0(\eta) \log x + \frac{1}{2\,\pi^2} \tilde{K}_1(\eta) \log x^2 \right] . \tag{3.23}$$

Substituting (3.5), (3.23) and (3.20) into (2.6) and retaining terms of $0(\varepsilon^2)$, the following ordinary differential equations result

$$\tilde{L}_0''' + f \tilde{L}_0'' + f'' \tilde{L}_0 = 2 f' \tilde{K}_0' - 2 f'' \tilde{K}_0 + 2 M_0' \tilde{N}_0' - 2 \tilde{N}_0'' M_0 , \tag{3.24a}$$

with $\tilde{L}_0(0) = \tilde{L}_0'(0) = \tilde{L}_0'(\infty) = 0$,

$$\tilde{K}_0''' + f \tilde{K}_0'' + f'' \tilde{K}_0 = 2 f' \tilde{K}_1' - 2 f'' \tilde{K}_1 + 2 M_0'^2 - \tilde{N}_0 M_0'' + 2 M_0 M_0'' - M_0 \tilde{N}_0'' - 4 , \tag{3.24b}$$

with $\tilde{K}_0(0) = \tilde{K}_0'(0) = 0$, $\tilde{K}_0'(\infty) = 1$,

$$\tilde{K}_1''' + f \tilde{K}_1'' + f'' \tilde{K}_1 = -2 M_0 M'' , \tag{3.24c}$$

with $\tilde{K}_1(0) = \tilde{K}_1'(0) = 0$, $\tilde{K}_1'(\infty) = 1$.

The streamwise velocity becomes

$$u = f'(\eta) + \frac{\varepsilon}{\pi}\left[\log x\, M_0'(\eta) + \tilde{N}_0'(\eta)\right] + \frac{\varepsilon^2}{\pi^2}\left[\tilde{L}_0'(\eta) + \log x\, \tilde{K}_0'(\eta) + \frac{\log^2 x}{2}\tilde{K}_1'(\eta)\right], \tag{3.25}$$

and the non-dimensional skin-friction coefficient is

$$\frac{C_f}{2}\sqrt{Re_\infty} = \frac{1}{\sqrt{2x}}\left\{f''(0) + \frac{\varepsilon}{\pi}\left[\log x\, M_0''(0) + \tilde{N}_0''(0)\right] + \frac{\varepsilon^2}{\pi^2}\left[\tilde{L}_0''(0) + \log x\, \tilde{K}_0''(0) + \frac{\log^2 x}{2}\tilde{K}_1''(0)\right]\right\}. \tag{3.26}$$

The 'exact' solution to this problem is the Falkner-Skan result, which as given in Rosenhead [5] is

$$\psi = \sqrt{2x}\left(\frac{x^m}{m+1}\right)^{1/2} F(\tilde{\eta}), \tag{3.27}$$

with

$$m = \frac{\varepsilon}{\pi}\left(1 - \frac{\varepsilon}{\pi}\right)^{-1},$$

$$\tilde{\eta} = Y(2x)^{-1/2}\left[(m+1)\, x^m\right]^{1/2}, \tag{3.28}$$

and F is the solution of

$$F'''(\tilde{\eta}) + F(\tilde{\eta})\, F''(\tilde{\eta}) + \frac{2\varepsilon}{\pi}\left[1 - F'(\tilde{\eta})^2\right] = 0, \tag{3.29}$$

with

$$F(0) = F'(0) = 0, \qquad F'(\infty) = 1.$$

The skin-friction coefficient becomes

$$\frac{C_f}{2}\sqrt{Re_\infty} = (2x)^{-1/2}\,(1 - \varepsilon/\pi)^{-1/2}\, x^{\left(\frac{3\,\varepsilon/2\,\pi}{1-\varepsilon/\pi}\right)} F''(0). \tag{3.30}$$

It is seen that the solution for small wedge angle determined in this analysis may have been determined directly from the Falkner-Skan result (3.27) and (3.29) by expanding about $\varepsilon = 0$. This technique is presented in Ref. [13] and by comparing with those results it is seen that

$$\tilde{N}_0(\eta) = 1/2\left[\eta f'(\eta) - f(\eta) + 2\pi K(\eta)\right], \tag{3.31a}$$

$$\tilde{L}_0(\eta) = 1/8\left[\eta^2 f''(\eta) + \eta f'(\eta) - f(\eta) + 4\pi\left[(\eta K'(\eta) - K(\eta)\right] + 4\pi^2 M(\eta)\right], \tag{3.31b}$$

$$\tilde{K}_0(\eta) = 1/4\left[\eta^2 f''(\eta) + 3\eta f'(\eta) + f(\eta) + 2\pi\left(\eta K'(\eta) + K(\eta)\right)\right], \tag{3.31c}$$

and

$$K_1(\eta) = 1/4\,[\eta^2 f''(\eta) + 3\,\eta f'(\eta) + f(\eta)]\,, \tag{3.31d}$$

where the functions of K and M are solutions of

$$K''' + f K'' + f'' K = -2/\pi\,[1 - f'^2]\,, \tag{3.31e}$$

with

$$K(0) = K'(0) = K'(\infty) = 0\,,$$

and

$$M''' + f M'' + f'' M = -\frac{8}{\pi} f' K' - 2 K K'' \tag{3.31f}$$

with $M(0) = M'(0) = M'(\infty) = 0$.

Solutions for (3.31e) and (3.31f) are tabulated in Table A-2. It is found that $K''(0) = 0.8269$ and $M''(0) = 1.2337$. The Libby-Fox [10] eigensolutions are also possible solutions for $\psi_i(x, y)$, but since the leading edge is sharp in the case of the wedge, they would only appear in higher-order boundary-layer considerations (in Reynolds number).

Velocity profiles and skin-friction coefficients are determined with (3.25) and (3.26). These results are plotted in Figures 7 through 9 for various values of x, the distance measured along the wedge, and a wedge angle of 9 degrees. Figures 7 and 8 depict the excellent agreement between the velocity profile calculated to order ε and the Falkner-Skan solution from equation (3.27). The skin-friction coefficients plotted in Figure 9 for the ε and ε^2 analyses are compared with the Falkner-Skan skin-friction coefficient, equation (3.30) and provide excellent agreement to order ε, with a slight improvement when the ε^2 terms are included. Figure 10 depicts the error in skin friction at $x = 1.0$ for a range of values of ε. It appears as if this method is quite

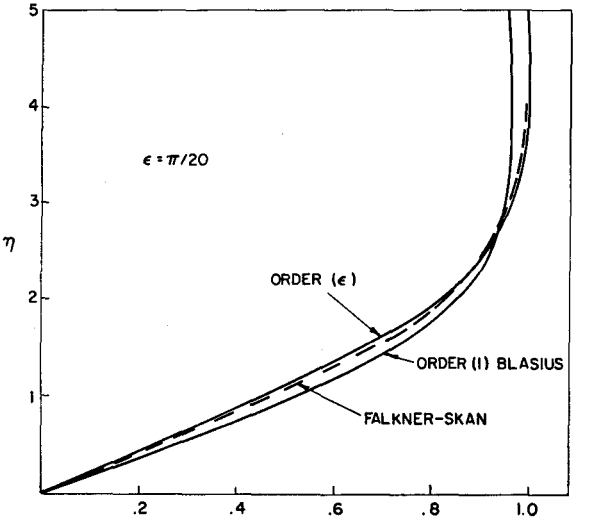

Figure 7
Velocity profile at $x = .5$ slender wedge.

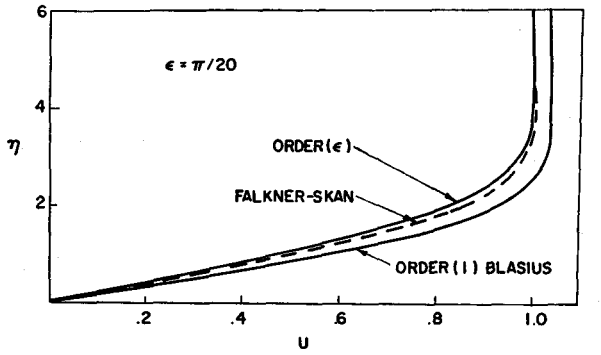

Figure 8
Velocity profile at $x = 2.0$ slender wedge.

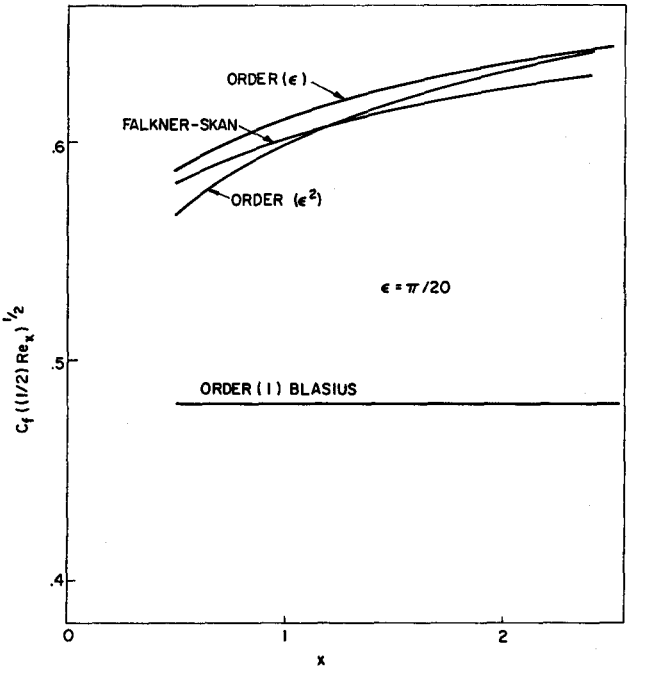

Figure 9
Skin friction vs. x, slender wedge.

satisfactory for $\varepsilon < 0.4$ or wedge angles of less than 20 degrees at this streamwise location. From Figure 9, with $\varepsilon/\pi = .05$, it is seen that this error is fairly uniform over a wide range of x.

4. Summary

A simple expansion method has been developed to calculate the laminar, incompressible boundary layer on thin airfoils. The results for the thin wedge illustrate the accuracy obtained by the techniques described herein and comparison with the 'exact' solution of Falkner-Skan is excellent. It has been found that excellent agreement for the velocity profile is obtained with only an order ε analysis, and a slight improvement in the values of skin friction results with the order ε^2 terms. The theory

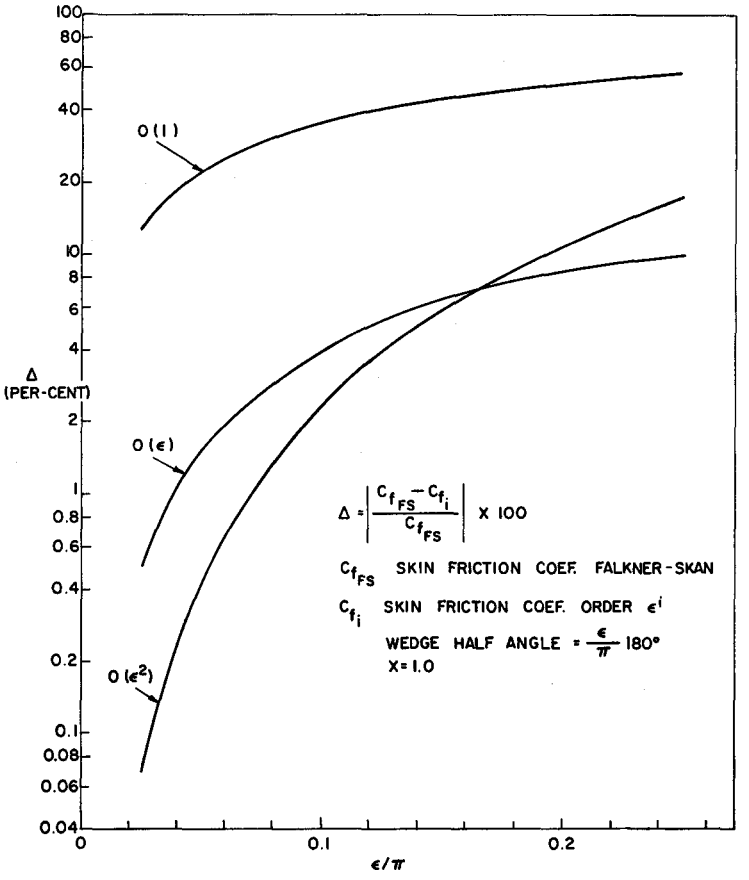

Figure 10
Skin friction error, slender wedge.

is good for wedge angles of less than 20 degrees at an intermediate streamwise location. The prediction of the location of the laminar separation point on the Joukowski airfoil confirms this result as agreement with a more exact numerical calculation is quite good. The method is applicable to any arbitrary airfoil shape having a blunt or sharp nose.

The techniques presented herein should be particularly useful in three-dimensional boundary-layer calculations where the linearized inviscid flow can be prescribed in terms of basic functions of x. The particular case of the flow transverse to a cruciform surface formed by the intersection of two thin wedges is considered in Ref. [8] and [13].

Appendix
Numerical Solutions or Ordinary Differential Equations

This appendix presents in tabular form solutions to the ordinary differential equations of the analysis. Typically the equations are third-order linear ordinary differential equations with variable coefficients. The boundary conditions are split over an infinite domain; that is, two conditions at η (the independent variable) equal

to zero and another condition applied as $\eta \to \infty$. As a consequence of the prescribed exponential decay of vorticity, all solutions are constrained to approach their asymptotic value, for large η, exponentially fast. Consider a typical equation

$$M_1'''(\eta) + f(\eta)\, M_1''(\eta) - 2 f'(\eta)\, M_1'(\eta) + 3 f''(\eta)\, M_1(\eta) = -2 \tag{A.1}$$

with the boundary conditions

$$M_1(0) = M_1'(0) = 0\,, \qquad M_1'(\infty) = 1$$

where $f(\eta)$ and $f'(\eta)$ are known functions.

The equation is solved by assuming a solution of the form

$$M_1(\eta) = C_1\, M_{1c}(\eta) + M_{1p}(\eta) \tag{A.2}$$

where C_1 is a constant, and M_{1c} and M_{1p} are respectively complementary and particular solutions to (A.1). Therefore,

$$M_{1_c}''' + f\, M_{1_c}'' - 2 f'\, M_{1_c}' + 3 f''\, M_{1_c} = 0\,, \tag{A.3}$$

with

$$M_{1_c}(0) = M_{1_c}'(0) = 0\,, \qquad M_{1_c}''(0) = 1\,,$$

and

$$M_{1p}'' + f\, M_{1p} - 2 f'\, M_{1p}' + 3 f''\, M_{1p} = -2\,, \tag{A.4}$$

with $M_{1p}(0) = M_{1p}'(0) = 0$, $M_{1p}''(0) = 1$.

Equations (A.3) and (A.4) are initial value problems and can be integrated numerically using standard techniques. The numerical solutions to (A.3) and (A.4) are substituted into (A.2) to determine the solution for $M_1(\eta)$. The one remaining asymptotic boundary condition $M_1(\infty) = 1$ must now be satisfied. The free constant in equation (A.1) is used to satisfy this condition at $\eta = 10$. Namely,

$$M_1'(10) = 1 = C_1\, M_{1c}'(10) + M_{1p}'(10)$$

or

$$C_1 = [1 - M_{1p}'(10)]/M_{1c}'(10).$$

It is important to note that for all of the equations considered here, the complementary and particular solutions have both exponentially decaying and algebraically growing parts but not algebraic decay; therefore, integration of M_{1c} and M_{1p} could be terminated at $\eta = 10$. Clearly this procedure would be considerably more complex if algebraic decay occurred. The final solution for $M_1(\eta)$ is

$$M_1(\eta) = \left[\frac{1 - M_{1p}'(10)}{M_{1c}'(10)}\right] M_{1c}(\eta) + M_{1p}(\eta)$$

as the algebraic growth has been filtered out. The method used to numerically integrate the equations was usually a Runge-Kutta technique with a step size of $\Delta\eta = 10^{-3}$.

Table A-1

Differential equations of section 2

η	$M_0'(\eta)$	$M_1'(\eta)$	$\bar{N}_0'(\eta)$	$\bar{N}_1'(\eta)$	$N_2'(\eta)$
.2	0.1408	0.5380	0.4039	− 0.1015	0.8206
.4	0.2811	0.9960	0.7665	− 0.1274	1.484
.6	0.4192	1.374	1.085	− 0.0875	1.999
.8	0.5527	1.672	1.354	0.0042	2.373
1.0	0.6782	1.892	1.570	0.1317	2.620
1.4	0.8911	2.106	1.827	0.4303	2.779
1.8	1.033	2.069	1.857	0.7016	2.599
2.2	1.096	1.841	1.714	0.8876	2.212
3.0	1.071	1.317	1.284	1.014	1.439
4.0	1.012	1.036	1.032	1.006	1.048
6.0	1.000	1.000	1.007	1.000	1.006
8.0	1.000	1.000	1.000	1.000	1.000

$M_0''(0) = 0.7044$, $M_1''(0) = 2.890$, $\bar{N}_0''(0) = 2.120$, $\bar{N}_1''(0) = -0.7062$, $N_2''(0) = 4.498$.

Table A-2

K and M, $K''' + f K'' + f'' K = -2/\pi\,(1 - f'^2)$, $M''' + f M'' + f'' M = -8/\pi f' K' - 2 K K''$.

η	K	K'	K''	M	M'	M''
0.0	0.0000	0.0000	0.8269	0.0000	0.0000	− 1.2337
.5	0.0900	0.3329	0.5015	− .1537	− .6118	− 1.1929
1.0	0.3049	0.4984	0.1603	− .6004	− 1.1510	− 0.9039
1.5	0.5608	0.4999	− 0.1389	− 1.2649	− 1.4519	− 0.2463
2.0	0.7848	0.3827	− 0.3009	− 1.9883	− 1.3769	0.5235
2.5	0.9373	0.2280	− 0.2933	− 2.5889	− 0.9919	0.9256
3.0	1.0185	0.1056	− 0.1892	− 2.9696	− 0.5412	0.8062
3.5	1.0523	0.0380	− 0.0873	− 3.1535	− 0.2238	0.4567
4.0	1.0633	0.0106	− 0.0298	− 3.2213	− 0.0705	0.1819
4.5	1.0661	0.0023	− 0.0076	− 3.2405	− 0.0170	0.0528
5.0	1.0666	0.0004	− 0.0015	− 3.2447	− 0.0031	0.0114
5.5	1.0667	0.0001	− 0.0002	− 3.2454	− 0.0004	0.0019
6.0	1.0667	.0000	− .0000	− 3.2455	− .0000	0.0002
6.5	1.0667	.0000	− .0000	− 3.2455	− .0000	.0000
7.0	1.0667	.0000	− .0000	− 3.2455	− .0000	.0000
7.5	1.0667	− .0000	− .0000	− 3.2455	− .0000	.0000
8.0	1.0667	− .0000	.0000	− 3.2455	− .0000	.0000
8.5	1.0667	− .0000	.0000	− 3.2455	− .0000	.0000
9.0	1.0667	− .0000	.0000	− 3.2455	− .0000	.0000
9.5	1.0667	− .0000	.0000	− 3.2455	− .0000	.0000

References

[1] M. J. Lighthill, *A New Approach to Thin Airfoil Theory*, Aero. Quart. *3*, 193 (1951).

[2] R. T. Jones and D. Cohen, *High Speed Wing Theory* (Princeton University Press, Princeton, N. J. 1960).

[3] M. Van Dyke, *Perturbation Methods in Fluid Mechanics* (Academic Press, New York 1964).

[4] H. Schlichting, *Boundary Layer Theory* (McGraw-Hill, New York 1960).

[5] L. Rosenhead, Editor, *Laminar Boundary Layers* (Oxford University Press, London 1963).

[6] A. MAGER, *Three-Dimensional Laminar Boundary Layer with Small Cross-Flow*, J. Aero. Sci. *21* (1954).
[7] W. W. WOOD, Ph. D. Dissertation (Cambridge University, 1955).
[8] B. GROSSMAN and S. G. RUBIN, *Viscous Flow Along a Corner, Part III: Effects of Axial Pressure Gradients* (Polytechnic Institute of Brooklyn, PIBAL Rept. No. 70-54, Dec. 1970.)
[9] K. STEWARTSON, *On Asymptotic Expansions in the Theory of Boundary Layers*, J. Math. Phys. *36*, 173 (1957).
[10] P. A. LIBBY and H. FOX, *Some Perturbation Solutions in Laminar Boundary-Layer Theory, Part I: The Momentum Equation*, J. Fluid Mech. *17*, 433 (1963).
[11] M. VAN DYKE, *Higher Approximations in Boundary-Layer Theory, Part 3: Parabola in Uniform Stream*, J. Fluid Mech. *19*, 145 (1964).
[12] W. YOUNG JR. and J. C. WILLIAMS III, *The Boundary Layer on Rotating Blades in Forward Flight*, AIAA 8th Aerospace Sci. Meeting, Paper No. 70-50, New York 1970.
[13] B. GROSSMAN, *Viscous Corner Flows*, Ph. D. Thesis (Polytechnic Institute of Brooklyn, 1969).

Zusammenfassung

Zur Untersuchung der laminaren inkompressiblen Grenzschicht an dünnen Profilen wird eine einfache Expansionsmethode angegeben. Diese Methode verbindet die Entwicklung für kleine Störungen mit den «quasi-ähnlichen» Theorien der Grenzschicht. Verschiedene geometrische Formen wurden behandelt, einschliesslich eines Joukowski-Profils, eines Parabel-Profils und eines schlanken Keils. Die erhaltenen Profile und Reibungswerte sind in guter Übereinstimmung mit Resultaten aus anderen Quellen, selbst für ziemlich dicke Profile. Die Anwendung der Methode dürfte besonders nützlich werden im drei-dimensionalen Fall, wo andere zwei-dimensionale Methoden nicht einfach übertragen werden können.

(Received: April 2, 1970; revised: September 28, 1970)

On Local Görtler Instability

By Murray Tobak, Ames Research Center, NASA, Moffett Field, California, USA

1. Introduction

The instability of boundary-layer flows over concave walls to perturbations in the form of longitudinal vortices was first demonstrated theoretically by Görtler [1] in 1940. Ever since detailed studies of the transition from laminar to turbulent flow revealed the necessary involvement of three-dimensional disturbances, Görtler's analysis, descriptive as it is of a three-dimensional instability, has held an important place in the development of ideas concerning the nature of laminar boundary-layer instability.

Although the predictions of the theory have been confirmed under experimental conditions approximating those assumed in the formulation [2–4] many of its implications have not been as fully explored because certain of the theoretical assumptions limit its applicability to an as yet undetermined degree. One such assumption is that the wall, of infinite streamwise extent, have a constant curvature everywhere along its length. In practice, wall curvature normally is present over only